Articles

Reactions of Diacetylene Ligands with Trinuclear Clusters. 3. Cyclization of Diynes with β-Amino Moieties on the Metal Core of $[H_2Os_3(CO)_{10}]$

Sergey P. Tunik,* Vassily D. Khripun, and Irina A. Balova

Department of Chemistry, St. Petersburg University, Universitetskii pr., 2, St. Petersburg, 198904, Russian Federation

Ebbe Nordlander*

Inorganic Chemistry 1, Chemical Center, Lund University, Box 124, SE-221 00 Lund, Sweden

Matti Haukka and Tapani A. Pakkanen

Department of Chemistry, University of Joensuu, P.O. Box 111, FIN-80101 Joensuu, Finland

Paul R. Raithby

Department of Chemistry, University of Cambridge, Lensfield Road, Cambridge, CB2 1EW, U.K.

Received May 15, 2001

Reactions of $[H_2Os_3(CO)_{10}]$ with the substituted diynes $R-C_2-C_2-R'$ (**1**, R = Ph, R′ = CH_2NHPh; **2**, R = Ph, R′ = CH_2NHCH_2Ph; **3**, R = R′ = CH_2NHPh) afford the clusters $[HOs_3(CO)_{10}(L)]$ (L = {μ-η^1:η^2-$PhCH_2C(H)$═C−C(H)═C−NPh} (**4**), {μ-η^1:η^2-$PhCH_2C(H)$═C−C(H)═C−NCH_2Ph} (**5**), and {μ-η^1:η^1-CH_3CC═C−C(H)═C(H)−NPh} (**6**), which have been characterized by single-crystal X-ray diffraction analyses as well as by various spectroscopic methods. In clusters **4**−**6**, the starting diynes **1**−**3** have been rearranged to form substituted pyrrolyl rings which bridge two osmium atoms in η^1:η^2- (**4**, **5**) or η^1:η^1- (**6**) coordination modes depending on the nature of substituents in **1**−**3**. A possible reaction pathway for the diyne cyclization reactions that yield **4**−**6** involves initial transfer of a hydride onto a coordinated diyne followed by a series of 1,3-shifts and subsequent nucleophilic attack of the nitrogen on the third carbon atom of the diyne system to afford the five-membered pyrrolyl ring. Cluster **6** and its previously characterized furanyl analogue $[HOs_3(CO)_{10}\{\mu$-η^1:η^1-(OCH-CHCC)−C−$CH_3)\}]$ (**7**) undergo facile thermal transformation accompanied by the loss of a CO ligand to give the clusters $[HOs_3(CO)_9\{\mu_3,\eta^3$-$CH_3CC$═C−C(H)═C(H)−NPh}] (**8**) and $[HOs_3(CO)_9\{\mu_3,\eta^3$-(OCH═CHC═CCC$H_3)\}]$ (**9**). In both **8** and **9**, single-crystal X-ray analysis revealed the presence of pentagonal pyramid cluster cores containing three osmium and three carbon atoms.

Introduction

Reactions of 1,3-conjugated diynes with osmium and ruthenium carbonyl clusters have attracted considerable attention due to the unusual transformations which the ligands undergo in these reactions.[1−7] In recent publications[5,6] we have shown that several diynes tend to rearrange to yield coordinated five-membered rings when reacted with $[H_2Os_3(CO)_{10}]$. An important feature of these reactions is that the cyclization appears to proceed through abstraction of a hydrogen atom from

* Corresponding authors. E-mail for S.P.T.: stunik@st1323.spb.edu. E-mail for E.N.: Ebbe.Nordlander@inorg.lu.se.

(1) Deeming, A. J.; Felix, M. S. B.; Bates, P. A.; Hursthouse, M. B. *J. Chem. Soc., Chem. Commun.* **1987**, 461.

(2) (a) Corrigan, J. F.; Doherty, S.; Taylor, N. J.; Carty, A. J. *Organometallics* **1992**, *11*, 3160. (b) Corrigan, J. F.; Taylor, N. J.; Carty, A. J. *Organometallics* **1994**, *13*, 3778. (c) Blenkiron, P.; Taylor, N. J.; Carty, A. J. *J. Chem. Soc., Chem. Commun.* **1995**, 327.

(3) (a) Bruce, M. I.; Zaitseva, N. N.; Skelton, B. W.; White, A. H. *Inorg. Chim. Acta* **1996**, *250*, 129. (b) Bruce, M. I.; Zaitseva, N. N.; Skelton, B. W.; White, A. H. *J. Organomet. Chem.* **1997**, *536*−*537*, 93. (c) Bruce, M. I.; Skelton, B. W.; White, A. H.; Zaitseva, N. N. *J. Organomet. Chem.* **1998**, *558*, 197. (d) Bruce, M. I.; Skelton, B. W.; White, A. H.; Zaitseva, N. N. *Inorg. Chem. Commun.* **1998**, *1*, 134.

(4) Tunik, S. P.; Grachova, E. V.; Denisov, V. R.; Starova, G. L.; Nikol'skii, A. B.; Dolgushin, F. M.; Yanovskii, A. I.; Struchkov, Yu. T. *J. Organomet. Chem.* **1997**, *536*−*537*, 339.

(5) Karpov, M. G.; Tunik, S. P.; Denisov, V. R.; Starova, G. L.; Nikol'skii, A. B.; Dolgushin, F. M.; Yanovskii, A. I.; Struchkov, Yu. T. *J. Organomet. Chem.* **1995**, *485*, 219.

(6) Clarke, L. P.; Davies, J. E.; Raithby, P. R.; Shields, G. P.; Tunik, S. P.; Krupenya, D. V.; Starova, G. L. *J. Chem. Soc., Dalton Trans.*, submitted for publication.

(7) Lau, C. S.-W.; Wong, W.-T. *J. Chem. Soc., Dalton Trans.* **1999**, 2511.

10.1021/om010400a CCC: $20.00
Publication on Web 07/31/2001

the β-atom of the diyne substituent coupled with the formation of a bond between the β-atom and the third carbon (relative to the substituent) of the $-C_2-C_2-$ diyne moiety. This process results in the formation of a pseudo-furan heterocycle in the case of $HOCH_2-C_2C_2-CH_2OH$[5] and an indenyl fragment in the case of $Ph-C_2-C_2-Ph$.[6] In the present study, we have examined the reactions of $[H_2Os_3(CO)_{10}]$ with diynes containing substituents with NH groups in β-position, at ambient temperature, as well as thermal transformations of the products generated in these reactions. The crystal and molecular structures of the new compounds obtained and possible pathways for these reactions are reported below.

Experimental Section

General Comments. The starting materials $[H_2Os_3(CO)_{10}]$,[8] $[HOs_3(CO)_{10}(OCH{=}CHC{=}CCCH_3)]$,[5] phenyl(5-phenyl-2,4-pentadiynyl)amine (**1**),[9a] benzyl(5-phenyl-2,4-pentadiynyl)-amine (**2**),[9a] and *N*,*N*-diphenyl-2,4-hexadiyne-1,6-diamine (**3**)[9b] were prepared according to published procedures. The deuterated cluster $[D_2Os_3(CO)_{10}]$ was obtained by direct reaction of gaseous D_2 and $[Os_3(CO)_{10}(NCMe)_2]$, which gave ca. 90% deuterium enrichment of the starting cluster. All solvents—dichloromethane, chloroform, hexane and diethyl ether (KEBO)—were distilled over appropriate drying agents under an atmosphere of nitrogen before use. Infrared spectra were recorded using a Nicolet Avatar 360 FTIR spectrometer. Fast atom bombardment (FAB+) mass spectra were obtained on a JEOL SX-102 instrument; 3-nitrobenzyl alcohol was used as a matrix and CsI as the calibrant. The isotopic distribution patterns observed in the mass spectra fit completely to the calculated patterns. ^{1}H NMR spectra were recorded on a Varian Unity 300 MHz spectrometer and ^{13}C NMR on a Bruker AM 500 instrument using $[Cr(acac)_3]$ as a relaxation agent, 20 mg per 4 mL of $CDCl_3$. Solvent resonances were used as internal standards. Thin-layer chromatography was performed on commercial plates precoated with Merck Kieselgel 60 to 0.5 mm thickness. Microanalyses were carried out in the Analytical Laboratories of St. Petersburg State University and University of Joensuu.

Reaction of $[H_2Os_3(CO)_{10}]$ with 1. $[H_2Os_3(CO)_{10}]$ (201.6 mg, 0.237 mmol) and $PhC_2C_2CH_2NHPh$ (**1**) (111.4 mg, 0.482 mmol) were dissolved in 10 cm^3 of dichloromethane and stirred overnight at room temperature. After removal of the solvent, the residue was dissolved in a minimum amount of CH_2Cl_2 and separated by preparative TLC using a hexane/chloroform mixture (4:1, v/v) as eluent. The main product was isolated as a dark red solid, $[HOs_3(CO)_{10}\{\mu\text{-}\eta^1{:}\eta^2\text{-}PhCH_2C(H){=}C{-}C(H){=}C{-}NPh\}]$ (**4**), R_f 0.39, 93.7 mg, 36.6% with respect to $[H_2Os_3(CO)_{10}]$. Anal. Calcd for $C_{27}H_{15}NO_{10}Os_3$ (1084.01): C, 29.92; H, 1.39; N, 1.29. Found: C, 30.00; H, 1.34; N, 1.34. IR (CH_2Cl_2, cm^{-1}): ν_{CO} 2097 w, 2055 vs, 2041 m, 2009 vs, 2001 sh, 1974 w. ^{1}H NMR ($CDCl_3$): 7.24−6.92 (m, 10H, phenyl), 7.73, 6.88 (AB protons of the pyrrolyl ring, J = 3 Hz), 3.95 (s, 2H, CH_2), −15.10 (s, 1H, μ-*H*Os). FAB-MS (*m*/*z*): 1083 [M$^+$] (Os$_3$ = 570) and [M$^+$ − *n*CO], *n* = 1−10. Single crystals of **4** suitable for X-ray analysis were grown from a pentane solution at 4 °C.

Reaction of $[H_2Os_3(CO)_{10}]$ with 2. $[H_2Os_3(CO)_{10}]$ (100 mg, 0.12 mmol) and $PhCH_2NHCH_2C_2C_2Ph$ (**2**) (61 mg, 0.25 mmol) were dissolved in 10 cm^3 of dichloromethane and stirred overnight at room temperature. The solvent was removed in vacuo, and the resultant residue was dissolved in a minimum amount of CH_2Cl_2 and separated by preparative TLC using a pentane/diethyl ether mixture (4:1, v/v) as eluant. The main product was isolated as a dark red solid, $[HOs_3(CO)_{10}\{\mu\text{-}\eta^1{:}\eta^2\text{-}PhCH_2C(H){=}C{-}C(H){=}C{-}NCH_2Ph\}]$ (**5**), R_f 0.50, 60.4 mg, 45.9%. Anal. Calcd for $C_{28}H_{17}NO_{10}Os_3$ (1098.04): C, 30.63; H, 1.56; N, 1.28. Found: C, 30.91; H, 1.76; N, 1.00. IR (CH_2Cl_2, cm^{-1}): ν_{CO} 2096 w, 2054 vs, 2042 m, 2008 vs, 1995 m,sh, 1979 m, 1966 w,sh. ^{1}H NMR ($CDCl_3$): 7.38−6.86 (m, 10H, phenyl), 7.74, 6.97 (AB protons of pyrrolyl ring, J = 3 Hz), 4.75 (s, 2H, CH_2), 3.89 (s, 2H, CH_2), −15.22 (s, 1H, μ-*H*Os). FAB-MS (*m*/*z*): 1097 [M$^+$] (Os$_3$ = 570) and [M$^+$ − *n*CO], *n* = 1−10. Single crystals of **5** suitable for X-ray analysis were grown from a heptane solution at 4 °C.

Reaction of $[H_2Os_3(CO)_{10}]$ with 3. $[H_2Os_3(CO)_{10}]$ (221.5 mg, 0.26 mmol) and $PhNHCH_2C_2C_2CH_2NHPh$ (**3**) (107.5 mg, 0.413 mmol) were dissolved in 20 cm^3 of dichloromethane and stirred overnight at room temperature. The solvent was removed in vacuo, and the resultant residue was dissolved in a minimum amount of CH_2Cl_2 and separated by preparative TLC using a hexane/dichloromethane mixture (4:1, v/v) as eluant. The main product was isolated as a cherry-red solid, $[HOs_3(CO)_{10}\{\mu\text{-}\eta^1{:}\eta^1\text{-}CH_3CC{=}C{-}C(H){=}C(H){-}NPh\}]$ (**6**), R_f 0.45, 115.3 mg, 43.5%. Anal. Calcd for $C_{22}H_{11}NO_{10}Os_3$ (1019.93): C, 25.91; H, 1.09; N, 1.37. Found: C, 26.68; H, 1.43; N, 1.42. IR (CH_2Cl_2, cm^{-1}): ν_{CO} 2097 w, 2057 vs, 2044 m, 2010 vs, 1999 sh, 1981 m. ^{1}H NMR ($CDCl_3$): 7.39 (m, 3H) and 7.1 (m, 2H), signals of phenyl ring protons; 7.28 (d, J = 3 Hz, 1H), 6.76 (d, J = 3 Hz 1H), signals of pyrrolyl ring protons bonded to C(15) and C(14), respectively; 2.31 (s, 3H, CH_3); −14.31 (s, 1H, μ-*H*Os). FAB-MS (*m*/*z*): 991 [M$^+$] (Os$_3$ = 570) and [M$^+$ − *n*CO], *n* = 1−9. Single crystals of **6** suitable for X-ray analysis were grown from a heptane solution at 4 °C.

Evolution of aniline in the course of this reaction has been detected by a standard analytical test (reaction with salicylaldehyde) for the presence of primary amines.[9c] The final reaction mixture obtained from 40 mg of $[H_2Os_3(CO)_{10}]$ and 12 mg of **3** was treated with 10 mg of salicylaldehyde. The Schiff base formed in the reaction mixture was compared with independently prepared 2-[(phenylimino)methyl]phenol to give identical TLC spot test retention parameters that unambiguously proved the formation of aniline in the reaction under study.

Reaction of $D_2Os_3(CO)_{10}$ with 3. $[D_2Os_3(CO)_{10}]$ (ca. 90% deuterium enrichment) (40 mg, 0.047 mmol) and $PhNHCH_2C_2C_2CH_2NHPh$ (**3**) (18 mg, 0.07 mmol) were dissolved in 2 cm^3 of dichloromethane and stirred overnight at room temperature. Separation of the reaction mixture was carried out as described above to give 21 mg of **6**. ^{1}H NMR ($CDCl_3$): 7.39 (m, 3H) and 7.1 (m, 2H), − signals of phenyl ring protons; 7.28 (s, *relative intensity* ***1.0***), 6.76 (d, J = 3 Hz, *relative intensity* ***0.1***), signals of pyrrolyl ring protons bonded to C(15) and C(14), respectively; 2.31 (s, ***3H***, CH_3); −14.31 (s, *relative intensity* ***0.1***, μ-*H*Os).

Conversion of the Complex 6 into $[HOs_3(CO)_9\{\mu_3,\eta^3\text{-}CH_3CC{=}C{-}C(H){=}C(H){-}NPh\}]$ (8). Compound **6** (25 mg, 0.025 mmol) was heated in refluxing $CHCl_3$ for 6 h. By this time, a TLC spot test showed complete consumption of **6**. The solvent was removed, and the residue was dissolved in a minimum amount of CH_2Cl_2 and separated by preparative TLC using a hexane/dichloromethane mixture (5:1, v/v) mixture as eluant. The main product was isolated as a yellow solid, $[HOs_3(CO)_9\{\mu_3,\eta^3\text{-}CH_3CC{=}C{-}C(H){=}C(H){-}NPh\}]$ (**8**), R_f 0.45, 20.6 mg, 85.1%. Anal. Calcd for $C_{21}H_{11}NO_9Os_3$ (991.92): C, 25.43; H, 1.12; N, 1.41. Found: C, 25.83; H, 1.27; N, 1.50. IR (CH_2Cl_2, cm^{-1}): ν_{CO} 2091 m, 2063 vs, 2038 s, 2008 vs, 1993 m, 1975 m,sh. ^{1}H NMR ($CDCl_3$): 7.24−6.92 (m, 5H, phenyl), 7.41 (d, 1H, J = 3.3 Hz), 6.62 (d, 1H, J = 3.3 Hz), 2.71 (s, 3H, CH_3), −19.44 (s, 1H, μ-*H*Os). FAB-MS (*m*/*z*): 963 [M$^+$] (Os$_3$ = 570) and [M$^+$ − *n*CO], *n* = 1−9. Single crystals of **8** suitable for X-ray analysis were grown from a heptane solution at 4 °C.

Conversion of the Complex 7 into $[HOs_3(CO)_9\{\mu_3,\eta^3\text{-}(OCH{=}CHC{=}CCCH_3)\}]$ (9). $[HOs_3(CO)_{10}\{\mu\text{-}\eta^1{:}\eta^1\text{-}(OCH{=}$

(8) Kaesz, H. D.; Knox, S. A. R.; Koepke, J. W.; Saillant, R. B. *J. Chem. Soc., Chem. Commun.* **1971**, 477.
(9) (a) Chodkiewicz, W.; Cadiot, P.; Willemart, A. *C. R. Acad. Sci., Ser. II*, **1956**, 241. (b) Hey A. S. *J. Org. Chem*. **1962**, 3320. (c) Johnson, J. B. *Anal. Chem*. **1956**, *28*, 1977.

Table 1. Crystal Data and Structure Refinement Details for Complexes 4−6, 8, and 9

	4	5	6	8	9
empirical formula	$C_{27}H_{15}NO_{10}Os_3$	$C_{28}H_{17}NO_{10}Os_3$	$C_{22}H_{11}NO_{10}Os_3$	$C_{21}H_{11}NO_9Os_3$	$C_{15}H_6O_{10}Os_3$
fw	1084.00	1098.03	1019.92	991.91	916.80
temp, K	120(2)	120(2)	120(2)	120(2)	120(2)
wavelength, Å	0.71073	0.71073	0.71073	0.71073	0.71073
cryst syst, space group	monoclinic, $P2_1$	orthorhombic, *Pbca*	monoclinic, $P2_1/n$	monoclinic, $P2_1/n$	monoclinic, $P2_1/c$
unit cell dimens					
a, Å	8.54650(10)	12.9812(2) Å	9.3557(2)	11.6596(2)	8.8466(2)
b, Å	17.3428(3)	15.6490(2) Å	20.7377(4)	16.6280(4)	16.7268(6)
c, Å	10.2360(2)	28.5971(5) Å	12.9452(2)	12.1008(2)	13.0923(5)
α, deg	90	90	90	90	90
β, deg	112.2990(10)	90	109.2830(10)	102.8370(10)	104.207(2)
γ, deg	90	90	90	90	90
volume, Å^3	1403.72(4)	5809.29(15)	2370.67(8)	2287.42(8)	1878.08(11)
Z, calcd density, Mg/m^3	2, 2.565	8, 2.511	4, 2.858	4, 2.880	4, 3.242 Mg/m^3
abs coeff, mm^{-1}	13.602	13.148	16.097	16.676	20.298
F(000)	984	4000	1832	1776	1616
cryst size, mm	0.30 × 0.30 × 0.10	0.30 × 0.20 × 0.10	0.20 × 0.20 × 0.20	0.30 × 0.20 × 0.10	0.20 × 0.10 × 0.05
θ range for data collection, deg	2.15−24.99	2.95−25.05	3.03−25.00	3.66−27.00	3.70−25.05
limiting indices	$-10\le h\le 10$, $-20\le k\le 20$, $-12\le l\le 12$	$-15\le h\le 15$, $-18\le k\le 18$, $-34\le l\le 34$	$-11\le h\le 11$, $-24\le k\le 24$, $-15\le l\le 15$	$-14\le h\le 14$, $-21\le k\le 21$, $-15\le l\le 15$	$-9\le h\le 10$, $-19\le k\le 19$, $-15\le l\le 15$
no. of reflns collected/ unique	13 686/4935 [*R*(int) = 0.0300]	41 760/5087 [*R*(int) = 0.0479]	25 788/4161 [*R*(int) = 0.0608]	28 889/4979 [*R*(int) = 0.0399]	24 948/3317 [*R*(int) = 0.0594]
abs corr	semiempirical from equivalents				
max. and min. transmn	0.3433 and 0.1057	0.3531 and 0.1103	0.2479 and 0.1022	0.2864 and 0.0820	0.4301 and 0.1064
refinement method	full-matrix least-squares on F^2				
no. of data/restraints/ params	4935/1/391	5087/0/379	4161/0/326	4979/0/312	3317/0/254
goodness-of-fit on F^2	1.043	1.185	1.066	1.128	1.230
final *R* indices [$I>2\sigma(I)$]	R1 = 0.0166, wR2 = 0.0385	R1 = 0.0340, wR2 = 0.0701	R1 = 0.0312, wR2 = 0.0791	R1 = 0.0208, wR2 = 0.0419	R1 = 0.0321, wR2 = 0.0642
R indices (all data)	R1 = 0.0172, wR2 = 0.0387	R1 = 0.0424, wR2 = 0.0727	R1 = 0.0350, wR2 = 0.0813	R1 = 0.0251, wR2 = 0.0434	R1 = 0.0414, wR2 = 0.0676
largest diff peak and hole, e/Å^{-3}	0.923 and −0.602	2.189 and −1.000	2.402 and −1.359	0.764 and −1.083	1.037 and −1.215

CHC═CCCH$_3$)}] (**7**) (50 mg, 0.054 mmol) was dissolved in 10 cm^3 of heptane, and the solution was heated at 80 °C for 30 min under a flow of argon. The color of the solution changed from deep red to yellow. The solvent was removed; the resultant residue was dissolved in a minimum amount of CH_2Cl_2 and separated by preparative TLC using hexane as eluant. The main product was isolated as a yellow solid, [$HOs_3(CO)_9$-{μ_3,η^3-(OCH═CHC═CCCH$_3$)}] (**9**), R_f 0.30, 43 mg, 87%. Anal. Calcd for $C_{15}H_6O_{10}Os_3$ (916.80): C, 19.65; H, 0.66. Found: C, 19.82; H, 0.84. IR (CH_2Cl_2, cm^{-1}): ν_{CO} 2098 m, 2070 vs, 2048 s, 2020 vs, 2008 sh, 2002 s, 1988 w, 1964 vw. ^{1}H NMR ($CDCl_3$): 7.98 (d, 1H, J = 1.5 Hz), 6.78 (d, 1H, J = 1.5 Hz), 3.13 (s, 3H, CH_3), −20.01 (s, 1H, μ-*H*Os). ^{13}C NMR ($CDCl_3$, 298 K): 179.4 (1 CO), 178.7 (1 CO), 174.6 (4 CO), 173.1 (1 CO), 171.8 (2 CO), 153.2 (dd, ^1J = 201 Hz, ^3J = 12 Hz, C(15)), 147.1 (m, C(13)), 140.9 (m, C(11)), 136.2 (m, C(12)), 126.0 (dd, ^1J = 180 Hz, ^3J = 12 Hz, C(14), 33.6 (q, ^1J = 128 Hz, C(16)). FAB-MS (*m*/*z*): 894 [M$^+$] (Os$_3$ = 570) and [M$^+$ − *n*CO], *n* = 1−6. Single crystals of **9** suitable for X-ray analysis were grown from heptane solution at 4 °C.

X-ray Data Collection and Structure Solution. X-ray diffraction data were collected with a Nonius Kappa CCD diffractometer using Mo Kα radiation (λ = 0.71073 Å) and ϕ-scan data collection mode with the Collect[10] collection program. The Denzo and Scalepack[11] programs were used for cell refinements and data reduction. Structures of **4**, **6**, **8**, and **9** were solved by direct methods or by the Patterson method using the SHELXS97 program.[12] The structure of **5** was solved by the Patterson method using the DIRDIF99 program.[13] A multiscan absorption correction, based on equivalent reflections (XPREP in SHELXTL v. 5.1),[14] was applied to all data (T_{max}/T_{min} was 0.3433/0.1057, 0.3531/0.1103, 0.2479/0.1022, 0.2864/0.0820, and 0.4301/0.1064 for **4**, **5**, **6**, **8**, and **9**, respectively). Structure refinements were carried out with the SHELXL97 program.[15] For compound **4** the phenyl hydrogens were constrained to ride on their parent atom (C−H = 0.95 Å, $U_{iso} = 1.2C_{eq}$). All other hydrogens were located from the difference Fourier map and refined isotropically. For compounds **5**, **6**, and **9** all hydrogens were placed in idealized positions (aromatic hydrogen: C−H = 0.95 Å, $U_{iso} = 1.2C_{eq}$, CH_2: C−H = 0.99 Å, $U_{iso} = 1.2C_{eq}$); the positions of hydrides were calculated using the XHYDEX program.[16] For compound **8** all organic hydrogens were placed in idealized positions (aromatic hydrogens: C−H = 0.95 Å, $U_{iso} = 1.2C_{eq}$, CH_3: C−H = 0.98 Å, $U_{iso} = 1.5C_{eq}$). The hydride was located from the difference Fourier map and refined isotropically. Crystallographic data are summarized in Table 1, and selected bond lengths and angles in Table 2.

Results and Discussion

The reactions of the amine-containing diynes $PhC_2C_2CH_2NHPh$ (**1**), $PhC_2C_2CH_2NHCH_2Ph$ (**2**), and $PhNHCH_2C_2C_2CH_2NHPh$ (**3**) with [$H_2Os_3(CO)_{10}$] result, in all three cases, in rearrangement of the diynes to

(10) *Collect*, data collection software; Nonius, 1999.
(11) Otwinowski, Z.; Minor, W. In *Methods in Enzymology*, *Volume 276*, *Macromolecular Crystallography, part A*; Carter, C. W., Jr., Sweet, R. M., Eds.; Academic Press: New York, 1997; pp 307−326.
(12) Sheldrick, G. M. *SHELXS97*, Program for Crystal Structure Determination; University of Göttingen, 1997.
(13) Beurskens, P. T.; Beurskens, G.; de Gelder, R.; Garcia-Granda, S.; Gould, R. O.; Israel, R.; Smits, J. M. M. *The DIRDIF-99 program system*; Crystallography Laboratory, University of Nijmegen: The Netherlands, 1999.
(14) Sheldrick, G. M. *SHELXTL* Version 5.1; Bruker Analytical X-ray Systems, Bruker AXS, Inc.: Madison, WI, 1998.
(15) Sheldrick, G. M. *SHELXL97*, Program for Crystal Structure Refinement; University of Göttingen, 1997.
(16) Orpen, A. G. XHYDEX. *J. Chem. Soc., Dalton Trans.* **1980**, 2509.

Table 2. Comparative Structural Parameters of $HOs_3(CO)_{(x)}(L)$ Clusters, $x = 10$ and 9 (for numbering scheme see Figures 1−5)

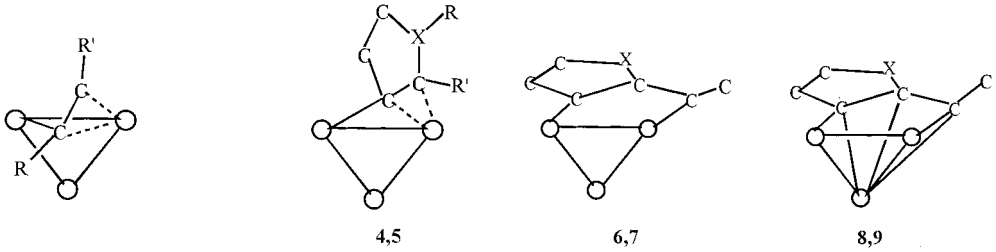

4,5 6,7 8,9

selected bond	$HOs_3(CO)_{10}$-$(HCCH_2)$[19]	$HOs_3(CO)_{10}$-(PhCCHPh)[21]	$HOs_3(CO)_{10}$-$(HCCH^tBu)$[20]	**4**	**5**	**6**	**7**[5]	**8**	**9**
Os(1)−Os(2)	2.845(2)	2.821(1)	2.834(1)	2.7694(3)	2.7762(4)	2.9424(4)	2.961(3)	2.9653(2)	3.0047(6)
Os(1)−Os(3)	2.857(2)	2.884(3)	2.858(1)	2.8943(3)	2.8584(4)	2.8991(4)	2.892(3)	2.8138(2)	2.8067(5)
Os(2)−Os(3)	2.917(2)	2.877(3)	2.923(1)	2.8833(3)	2.8859(4)	2.9022(4)	2.890(3)	2.8050(2)	2.8035(5)
Os(1)−C(13)	2.107(3)	2.15(5)	2.28(2)	2.280(6)	2.211(8)	2.095(7)	2.07(3)	2.078(4)	2.064(11)
Os(1)−C(12)	2.362(3)	2.45(1)	2.46(3)	3.111(5)	2.985(8)				
Os(2)−C(13)	2.273(3)	2.28(9)	2.15(2)	2.225(5)	2.282(8)				
Os(2)−C(11)						2.132(7)	2.00(3)	2.106(5)	2.087(11)
Os(3)−C(11)								2.281(4)	2.329(10)
Os(3)−C(12)								2.384(4)	2.305(9)
Os(3)−C(13)								2.359(4)	2.364(10)
C(12)−C(13)	1.396(3)	1.36(6)	1.40(3)	1.427(7)	1.417(12)	1.439(10)	1.24(5)	1.466(6)	1.422(15)
C(13)−C(14)				1.450(8)	1.448(11)	1.405(10)	1.54(4)	1.439(6)	1.453(15)
C(14)−C(15)				1.330(8)	1.360(11)	1.380(11)	1.32(8)	1.341(6)	1.305(18)
X−C(12)[a]				1.345(7)	1.342(10)	1.455(9)	1.46	1.416(5)	1.400(12)
X−C(15)[a]				1.387(7)	1.409(10)	1.337(10)	1.52	1.385(6)	1.477(16)
C(11)−C(12)						1.374(10)	1.47	1.425(6)	1.390(15)
Os(1)−C(1)				1.897(6)	1.887(10)	1.906(8)		1.898(5)	1.927(13)
Os(1)−C(2)				1.911(5)	1.919(9)	1.920(7)		1.911(5)	1.914(12)
Os(1)−C(3)				1.901(6)	1.916(9)	1.952(8)		1.950(5)	1.963(13)
Os(2)−C(4)				1.903(6)	1.899(9)	1.912(7)		1.904(5)	1.907(12)
Os(2)−C(5)				1.905(6)	1.931(9)	1.908(7)		1.895(5)	1.882(11)
Os(2)−C(6)				1.909(6)	1.911(9)	1.963(8)		1.951(5)	1.927(14)
Os(3)−C(7)				1.915(7)	1.917(9)	1.943(8)		1.917(5)	1.917(12)
Os(3)−C(8)				1.962(6)	1.955(9)	1.939(8)		1.887(5)	1.887(12)
Os(3)−C(9)				1.920(7)	1.915(9)	1.911(7)		1.913(5)	1.920(12)
Os(3)−C(10)				1.949(7)	1.964(9)	1.959(8)			

[a] X = N for **4**, **5**, **6**, **8**; X = O for **7**, **9**.

afford coordinated five-membered pyrrolyl-containing ligands. In each case, the five-membered ring is the result of the formation of a bond between the nitrogen atom of the secondary amine and the third carbon of the diyne chain. It is likely that this general feature arises from a common step in the three reactions (vide infra). However, the processes cannot be completely identical since the coordination modes of the pyrrolyl-containing ligands to the clusters differ between the different products.

Synthesis and Characterization of $[HOs_3(CO)_{10}\{\mu\text{-}\eta^1\text{:}\eta^2\text{-}(Ph{-}(NCHCHCC){-}CH_2Ph)\}]$ (4) and $[HOs_3(CO)_{10}\{\mu\text{-}\eta^1\text{:}\eta^2\text{-}(PhCH_2{-}(NCHCHCC){-}CH_2Ph)\}]$ (5). Reactions of $[H_2Os_3(CO)_{10}]$ with $PhC_2C_2CH_2NHPh$ (**1**) and $PhC_2C_2CH_2NHCH_2Ph$ (**2**) proceed smoothly at room temperature to give $[HOs_3(CO)_{10}\{\mu\text{-}\eta^1\text{:}\eta^2\text{-}(Ph\text{-}(NCHCH\text{-}CC)\text{-}CH_2Ph)\}]$ (**4**) and $[HOs_3(CO)_{10}\{\mu\text{-}\eta^1\text{:}\eta^2\text{-}(PhCH_2{-}(NCHCHCC){-}CH_2Ph)\}]$ (**5**) as main products, respectively. The solid-state structures of **4** and **5** have been determined by crystallographic analysis, and their molecular structures are shown in Figures 1 and 2; selected bond lengths and angles are given in Table 2. The pyrrolyl rings in **4** and **5** are coordinated to the "$HOs_3(CO)_{10}$" unit through one of the double bonds of the ring in a $\mu\text{-}\eta^1\text{:}\eta^2$-coordination mode ($\sigma,\pi$-alkenyl coordination, cf. Figures 1, 2). This bonding mode is well known for reactions of $[H_2Os_3(CO)_{10}]$ with alkynes,[17−20] where coordination of the alkyne and subsequent transfer of a hydride onto the alkyne gives rise to σ,π-alkenyl coordination. The orientation of the C_2 alkenyl fragment with respect to the Os−Os bond and other structural parameters of the Os_2C_2 fragment depend on the electronic properties and steric demands of the alkenyl moiety substituents and vary substantially in previously studied clusters.[17−20] A comparative analysis of the corresponding structural parameters shows that the bonding of the pyrrolyl fragment in clusters **4** and **5** is somewhat weaker than that observed for noncyclic alkenyls. The σ Os−C bond in **4** and **5** is elongated by ca. 0.12 and 0.10 Å, respectively, as compared with the sterically nondemanding vinyl ligand in $[HOs_3(CO)_{10}(\sigma,\pi\text{-}HCCH_2)]$.[18] The difference in coordination is particularly noticeable in the π-bonding where the longest Os(1)−C(12) bond reaches the value 3.111(5) Å in **4** and 2.985(8) Å in **5** as compared with 2.362 Å in $[HOs_3(CO)_{10}(\sigma,\pi\text{-}HCCH_2)]$. Due to the apparently high steric demands of the pyrrolyl ring substituents in **4** and **5**, the coordinated ligand is significantly shifted out of the osmium triangle, as is shown in the schematic figures

(17) Orpen, A. G.; Riera, A. V.; Bryan, E. G.; Pippard, D.; Sheldrick, G. M.; Rose, K. D. *J. Chem. Soc., Chem. Commun.* **1978**, 713.
(18) Guy, J. J.; Reichert, B. E.; Sheldrick, G. M. *Acta Crystallogr.* **1976**, *B32*, 3319.
(19) Clauss, A. D.; Tachikawa, M.; Shapley, J. R.; Pierpont, C. G. *Inorg. Chem.* **1981**, *20*, 1528.
(20) Sappa, E.; Tiripicchio, A.; Lanfredi, A. M. M. *J. Organomet. Chem.* **1983**, *249*, 391.

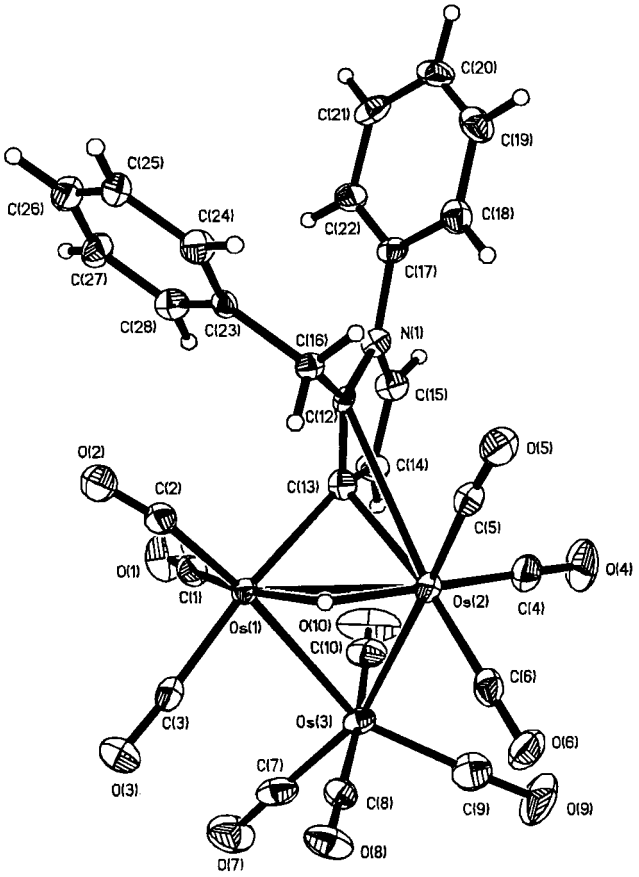

Figure 1. ORTEP plot of the molecular structure of $[HOs_3(CO)_{10}\{\mu\text{-}\eta^1\text{:}\eta^2\text{-}PhCH_2C(H)=C-C(H)=C-NPh\}]$, **4**. Thermal ellipsoids are drawn at the 50% probablility level.

attached to Table 2. This makes the π-interaction with the Os(1) atom rather weak; nevertheless, the presence of such bonding in the molecules discussed here is evident from the substantial elongation of the coordinated C(12)−C(13) double bond in the pyrrolyl ring as compared with the C(14)−C(15) double bond, which is not coordinated to a metal, cf. Table 2. The σ,π-coordination mode is also required by the EAN rule, as the alkenyl fragment should act as a three-electron donor in order to give rise to a stable 48-electron triangular cluster.

The averages of the three metal−metal bond distances in **4** and **5** are slightly shorter than those for related $[HOs_3(CO)_{10}(\text{alkenyl})]$ clusters,[17−19] the bridged Os(1)−Os(2) bond being the shortest metal−metal bond in each alkenyl cluster presented in Table 2. It is also worth noting that Os(1)−Os(2) bonds in **4** and **5** are systematically shorter (2.7694(3), 2.7762(4) Å, respectively) than those in the other alkenyl derivatives (2.845(2), 2.821(1), 2.834(1) Å, see Table 2). In contrast to this observation the other Os(1)−Os(3) and Os(2)−Os(3) bonds span the range 2.841−2.916 Å and do not display systematic variations within this group of compounds. The ^{1}H NMR resonances for the hydrides in **4** and **5** occur at −15.10 and −15.22 ppm, respectively, which are typical shifts for bridging hydrides in osmium carbonyl clusters. Analysis of the crystallographic electron density maps located the hydrides on the Os(1)−Os(2) edge in both clusters, in agreement with the determination of the hydride position in $[HOs_3(CO)_{10}(HC=CH_2)]$ by neutron diffraction.[18] The Os−C(O) bond lengths range from 1.897(6) to 1.962(6) and from 1.887(10) to 1.964(9) Å in **4** and **5**, respectively, which are typical values for 48-electron saturated Os_3 clusters. The ^{1}H NMR spectra of the pyrrolyl ligands in **4** and **5** display typical patterns consisting of phenyl multiplets, two signals for the protons from the pyrrolyl ring, and one methylene resonance in **4** and two in the case of **5** (cf. Experimental Section). These data are consistent with the solid-state structures, indicating that these structures are retained in solution for these clusters.

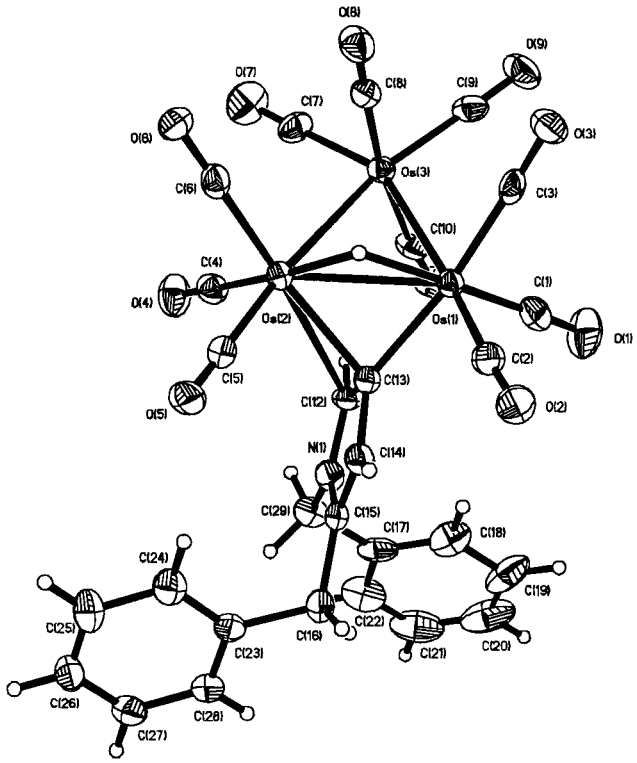

Figure 2. ORTEP plot of the molecular structure of $[HOs_3(CO)_{10}\{\mu\text{-}\eta^1\text{:}\eta^2\text{-}PhCH_2C(H)=C-C(H)=C-NCH_2Ph\}]$, **5**. Thermal ellipsoids are drawn at the 50% probability level.

Synthesis and Characterization of $[HOs_3(CO)_{10}\{\mu\text{-}\eta^1\text{:}\eta^1\text{-}(Ph-(NCHCHCC)-C-CH_3)\}]$ (6). The symmetrically substituted diyne $PhNHCH_2C_2C_2CH_2NHPh$ (**3**) reacts with $[H_2Os_3(CO)_{10}]$ to give $[HOs_3(CO)_{10}\{\mu\text{-}\eta^1\text{:}\eta^1\text{-}(Ph-(NCHCHCC)-C-CH_3)\}]$ (**6**), which contains a substituted pyrrolyl moiety similar to those found in **4** and **5**. The solid-state structure of **6**, which was determined by a single-crystal X-ray analysis, is shown in Figure 3; selected bond lengths and angles are given in Table 2. It appears that the pyrrolyl moiety has been formed by closure of the bond between a nitrogen atom of a substituent and the third carbon of the diyne chain, accompanied by C−N cleavage in the other substituent to eliminate aniline (vide infra). Evolution of aniline has been detected by the standard reaction with salicylaldehyde to form the Schiff base 2-[(phenylimino)methyl]-phenol. The identification of the Schiff base formed in the reaction mixture was made by a comparative TLC spot test, in which independently prepared 2-[(phenylimino)methyl]phenol was used as a standard. The molecular structure of **6** reveals that the pyrrolyl ring is coordinated in a manner that differs fundamentally from that found in **4** and **5**. The observed coordination mode is an example of a common $[HOs_3(CO)_{10}(\mu\text{-L})]$ bonding pattern where two osmium atoms are bridged

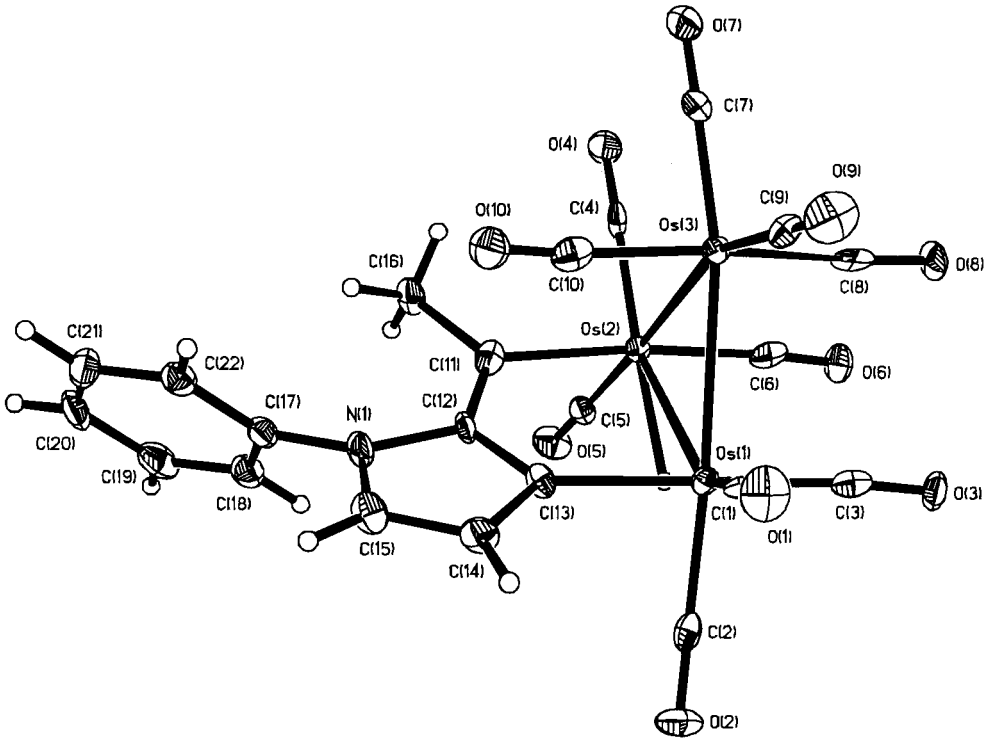

Figure 3. ORTEP plot of the molecular structure of $[HOs_3(CO)_{10}\{\mu\text{-}\eta^1\text{:}\eta^1\text{-}CH_3CC{=}C{-}C(H){=}C(H){-}NPh\}]$, **6**. Thermal ellipsoids are drawn at the 50% probability level.

by a chain of three ligand atoms. There are several examples of this type of bonding,[21] including the closely related structure $[HOs_3(CO)_{10}\{\mu\text{-}\eta^1\text{:}\eta^1\text{-}(OCHCHCC){-}C{-}CH_3)\}]$ (**7**), which is obtained by the reaction of $[H_2Os_3(CO)_{10}]$ with the $HOCH_2C_2C_2CH_2OH$ ligand with elimination of H_2O.[5] It appears that formation of the thermodynamically favored products like aniline and water may contribute to the stability of the ligand coordination modes found in **6** and **7**, respectively. The NMR and IR spectroscopic data confirm that the structure found in the solid state remains unchanged in solution. Two doublets at 7.28 and 6.76 ppm in the ^1H NMR spectrum of **6** were assigned to the pyrrolyl ring hydrogens bonded to C(15) and C(14), respectively. This assignment was based on the assumption that the hydrogen in the α (with respect to nitrogen) position displays lower field shift as compared with the remote β-hydrogen.

A comparison of the structures of **6** and **7** shows that both compounds contain three similar fragments, viz., a "$HOs_3(CO)_{10}$" core, a nitrogen/oxygen-containing five-membered heterocycle, and an "Os_2C_3" unit, which ties the former two fragments together. However, the heterocycles and the "Os_2C_3" units in **6** and **7** display some structural variations, which appear to result from the difference in the heteroatom. In both clusters, the coordinated organic ligands are formal three-electron donors in order to achieve the stable 48-electron cluster configurations required by the EAN rule. In the case of **7**, this requires the presence of a carbene, as is schematically shown in Scheme 1. The bond lengths found in the corresponding vinyl carbene fragments in **7** (cf. Table 2) are in agreement with an alteration of single

Scheme 1. Schematic Representation of Bonding in a Fragment of the Cluster 7

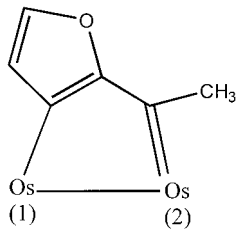

and double bonds, as shown in the drawing in Table 2. This indicates a negligible degree of delocalization of the double bonds in and between the furanyl and "diosmacyclopentadiene" fragments. In general, the degree of aromatization in furan derivatives is usually lower than that of corresponding pyrrolyl systems, this difference is assigned to a lesser involvement of the oxygen lone pairs in the π-system electron density delocalization.[22]

In contrast, crystallographic data for **6** (Table 2) indicate a considerable delocalization of double bonds. Whereas in **7** there are clear single−double bond alterations with C−C bond distances varying from 1.24 to 1.54 Å, there is very little variation in the corresponding distances of the pyrrolyl and "diosmacyclopentadiene" rings in **6**, where the C−C distances range from 1.374(10) to 1.439(10) Å. Furthermore, there is no substantial difference between the Os(1)−C(13) and Os(2)−C(11) bond lengths, which are approximately equal to 2.096(7) and 2.131(7) Å, respectively. In the valence bond approach, the delocalized bonding in the "diosmacyclopentadiene"−pyrrolyl system may be represented

(21) Deeming, A. J. *Adv. Organomet. Chem.* **1986**, *26*, 1.

(22) Gilchrist, T. L. *Heterocyclic Chemistry*, 2nd ed.; Longman Group UK Limited, London, 1992.

Scheme 2. Proposed Resonance Structures for 6

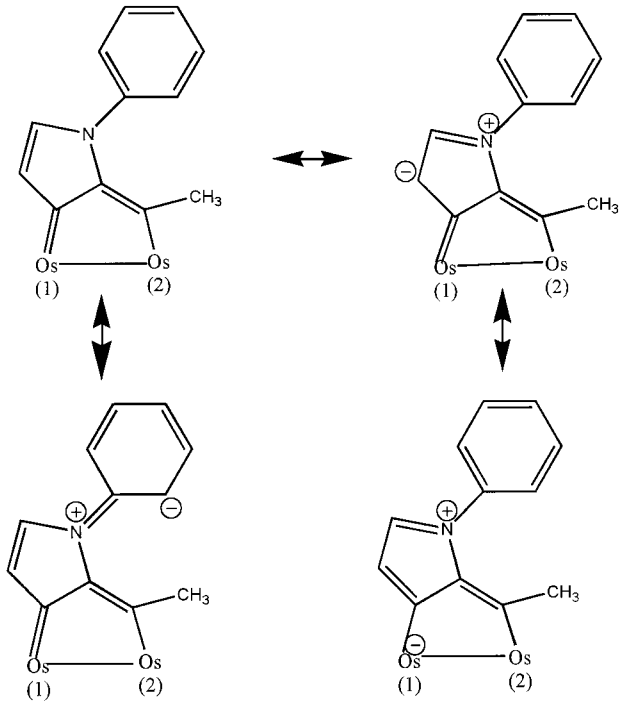

by the resonance structures shown in Scheme 2. These proposed resonance structures are compatible with the crystallographic data; in particular, this combination of resonance structures accounts for the shortening of the C(15)−N(1) and C(11)−C(12) bonds and lengthening of the C(12)−N(1) bond.

The osmium−osmium bond distances in **6** span the range 2.8991(4)−2.9424(4) Å. There are very small variations in the nonbridged Os−Os bond lengths in **4**, **5**, and **6**. The most substantial variations are observed for the Os(1)−Os(2) distances, which represent the Os−Os edge bridged by both the hydrocarbon and hydride ligands. In contrast to **4** and **5**, this is the longest Os−Os distance in **6**, most likely because of geometrical constraints inside the planar "diosmacyclopentadiene" ring, where the Os(1)−Os(2) distance should match the geometry of the C(11)−C(12)−C(13) fragment. This observation agrees with the structural features of **7**, where the same relative trend in the Os−Os bond distances is also observed (cf. Table 2).

Possible Reaction Pathways for Cyclization. The trend of diyne ligands to form five-membered cyclic systems when reacted with $[H_2Os_3(CO)_{10}]$ appears to be general for diynes containing a proton in γ-position of the ligand substituents.[5,6] The coordination modes of the rearranged ligands are dependent on the nature of the starting diynes. The following observations apply to all reactions studied to date.

(i) The reactions proceed via transfer of one hydride from $[H_2Os_3(CO)_{10}]$ onto the organic ligand, which is a general feature of the reaction products. The same diynes do **not** produce cyclic ligands in reactions with "nonhydride" clusters, e.g., $[M_3(CO)_{10}(NCMe)_2]$ (M = Ru, Os) or $[Ru_3(CO)_{12}]$.[1,3,4]

(ii) A short Os−C σ-bond that is found in all final products is most likely formed upon the initial hydride transfer and probably remains intact throughout the whole reaction.

(iii) The diynes forming cyclized products contain a nucleophilic center (nitrogen, oxygen) in the β-position of a substituent. The nucleophile is able to attack the third atom of the conjugated diyne chain in the cyclization process.

(iv) It is likely that the coordinated carbon chain serves as a channel for hydrogen atom movements, very probably through 1,3-shifts, to yield the hydrogen atom distribution observed in the final furanyl,[5] indenyl,[6] or pyrrolyl rings.

In an earlier paper,[6] we have suggested a reaction scheme for the interaction of $[H_2Os_3(CO)_{10}]$ with diphenyldiacetylene to produce $[HOs_3(CO)_{10}L]$ containing an indenyl fragment in the rearranged ligand (L). Similar reaction pathways, which are in agreement with the above-mentioned observations, are possible for the reactions involving the secondary amine diynes, **1**−**3**, discussed here; these pathways are shown in Scheme 3. The first step consists of the transfer of a hydride onto a ligand triple bond to generate an $[HOs_3(CO)_{10}\{\mu\text{-}\eta^1\text{:}\eta^2\text{-(alkenyl)}\}]$ cluster, which is well documented by the reactions of $[H_2Os_3(CO)_{10}]$ with monoalkynes under mild conditions.[17,19−21,23,24] This coordination mode results in bending of the initially linear $-C_2-C_2-$ fragment, thus facilitating cyclization of the ligand. It is plausible that this initial step is followed by a series of 1,3-hydrogen shifts to yield coordinated alkene−allenyl systems as shown in Scheme 3, setting the stage for closure of the five-membered ring by bringing the nucleophilic nitrogen in close proximity of the central carbon of the allenyl system. The driving force for the cyclization of the "enyl-yne" moiety is apparently so high that we have thus far failed to detect any intermediates in these reactions despite the fact that osmium clusters are relatively kinetically inert. The role of nitrogen as a nucleophilic center in the reactions studied is supported by the absence of any competitive cyclization to give an indenyl fragment similar to that found in the case of cyclization of diphenyldiacetylene in $[Os_3(\mu\text{-H})(CO)_{10}\{\mu_3,\eta^3\text{-(Ph(C)C}_9H_6)\}]$.[6] Cyclization into furan[25a,b] or thiazolidine [25c] rings through the attack of corresponding nucleophiles onto the central carbon atom of an allenyl system is well known in organic chemistry.

There is a substantial difference between the ligand coordination in, on one hand, **4** and **5**, and, on the other hand, in **6**. It is likely that this is due to the difference in the nature of the second ("noncyclized") substituent of **1**−**3**. Diynes **1** and **2** contain rather strong nonpolar C−C(ipso) bonds at the other end of the diyne. In these cases, the cyclization mechanism includes C(15)−N bond formation and transfer of a hydrogen atom onto the C(16) carbon to yield the pyrrolyl ring coordinated in the $\mu\text{-}\eta^1\text{:}\eta^2$-alkenyl mode. In **3**, the second substituent contains a polarized C−N bond, which can be cleaved in the attack of the nucleophilic nitrogen, as shown in Scheme 3. This reaction pathway is favored by the formation of a thermodynamically favorable aniline molecule and concomitant closure of the Os(2)−C(11)

(23) Deeming, A. J.; Hasso, S.; Underhill, M. *J. Chem. Soc., Dalton Trans.* **1975**, 1614.
(24) Tachikawa, M.; Shapley, J. R.; Pierpont, C. G. *J. Am. Chem. Soc.* **1975**, *97*, 7172.
(25) (a) Marshall, J. A.; Du Bay, W. J. *J. Org. Chem.* **1991**, *56*, 1686. (b) Marshall, J. A.; Du Bay, W. J. *J. Org. Chem.* **1994**, *59*, 1703. (c) Coen, S.; Ragonnet, B.; Vreillescazes, C.; Rogero, J. P. *Heterocycles* **1985**, *23*, 1225.

Scheme 3. Possible Mechanisms for the Cyclization of Ligands 1−3

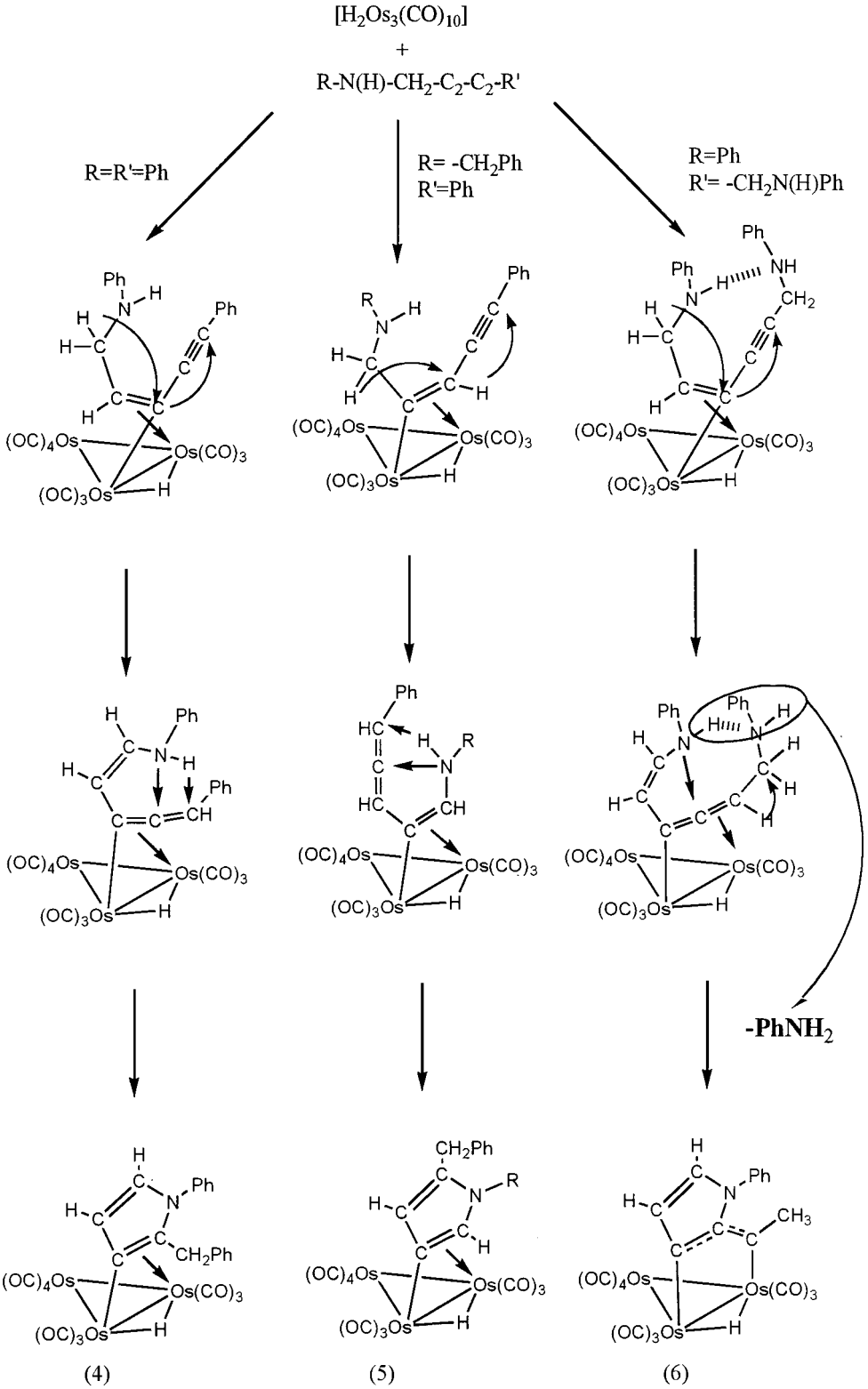

bond that results in η^3-bonding of the ligand to the Os(1)−Os(2) edge. The same reaction scheme can be applied to the reaction of $[H_2Os_3(CO)_{10}]$ with $OHCH_2C_2C_2CH_2OH$,[5] where the reaction sequence results in elimination of water and formation of a furanyl ring coordinated to the Os(1)−Os(2) edge in a μ-η^1:η^1-manner. To further prove the reaction scheme suggested, the synthesis of **6** starting from $[D_2Os_3(CO)_{10}]$ (ca. 90% deuterium enrichment, cf. Experimental Section) has been carried out. The isolated reaction product **6** displays the following ^{1}H spectrum: 7.39 (m, 3H) and 7.1 (m, 2H), phenyl ring protons; 7.28 (s, relative intensity 1.0), 6.76 (d, J = 3 Hz, relative intensity 0.1), 2.31 (s, 3H, CH_3); −14.31 (s, relative intensity 0.1, μ-*H*Os). The spectrum clearly indicates that (a) there is no D/H exchange for the hydride(s) during the reaction course and (b) the deuterium label is transferred into one position of the coordinated ligand

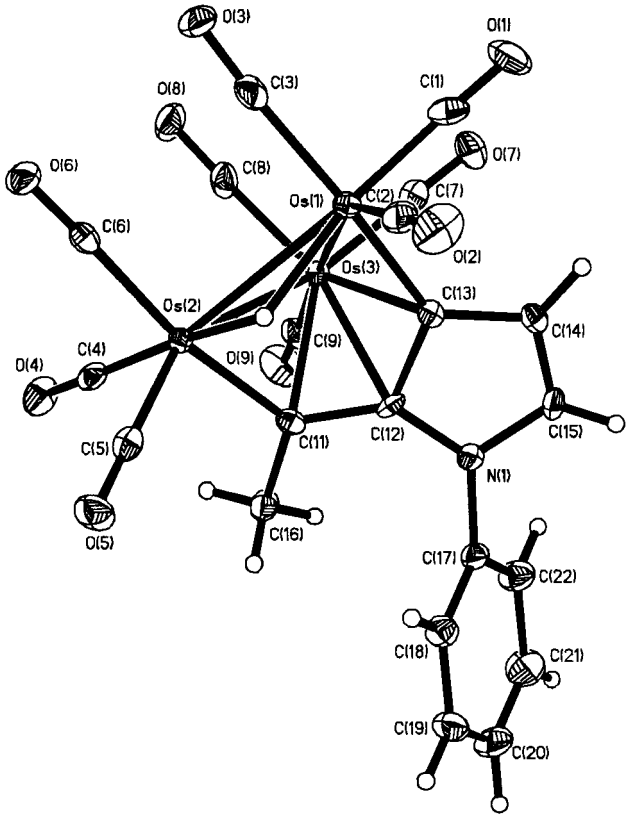

Figure 4. ORTEP plot of the molecular structure of $[HOs_3(CO)_9\{\mu_3,\eta^3\text{-}CH_3CC{=}C{-}C(H){=}C(H){-}NPh\}]$, **8**. Thermal ellipsoids are drawn at the 50% probability level.

exclusively, viz., onto C(14), cf. Figure 3. Both observations are in complete agreement with the reaction scheme proposed and imply that a reductive elimination/oxidative addition mechanism is a less feasible mechanism for the hydrogen shifts along the diyne chain.

Thermolysis of Clusters 6 and 7. Clusters **4** and **5** are thermally stable and remain intact on heating in boiling hexane solution for a few hours. In contrast, clusters **6** and **7** easily lose CO to give clusters **8** and **9**, respectively, the molecular structures of which are shown in Figures 4 and 5. Selected bond lengths and angles for both clusters are presented in Table 2. The main structural motif of the frameworks in **8** and **9** is a pentagonal pyramidal *nido* structure[26] formed by three osmium and three carbon atoms of the organic ligand. The EAN rule requires 58 electrons in order to provide the eight skeletal electron pairs required for stabilization of a six-vertex *nido* framework consisting of three transition metals and three p-block elements, which is in agreement with the number of valence electrons in **8** and **9**. This structural pattern is very common in the chemistry of alkyne-containing iron subgroup clusters[27] and appears to be a thermodynamic sink for the reactions of these complexes with alkynes. As has been pointed out above, the clusters **6** and **7** are characteristically different from **4** and **5** in their thermal reactivity, which can be accounted for by at least two obvious structural reasons. In both **6** and **7** the "diosmacyclopentadiene" ring (C(11)−C(12)−C(13)−Os(2)−Os(1) in

(26) Wade, K. *Adv. Inorg. Organomet. Chem.* **1976**, *18*, 1.
(27) Sappa, E. *J. Organomet. Chem.* **1999**, *573*, 139.

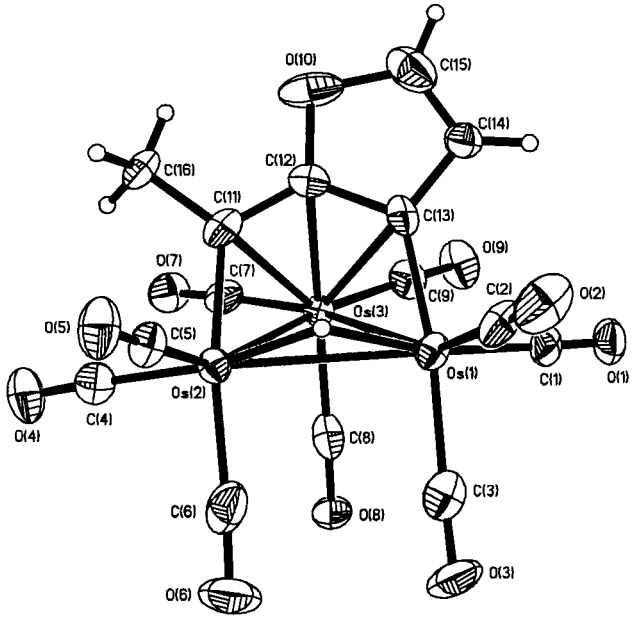

Figure 5. ORTEP plot of the molecular structure of $[HOs_3(CO)_9\{\mu_3,\eta^3\text{-}(OCH{=}CHC{=}CCCH_3)\}]$, **9**. Thermal ellipsoids are drawn at the 50% probability level.

6 (Figure 3) and the osmium triangle are structurally "prepared" fragments ready to form a stable pentagonal pyramid framework and therefore can easily afford a thermodynamically favorable framework. In the case of **4** and **5** (see Figures 1 and 2) only two carbon atoms of the ligand are involved in bonding to the Os(1)−Os(2) edge, which makes the transformation of this fragment into the pentagonal basal plane of the pyramid impossible and does not match any other stable configuration of a closed "Os_3C_2" framework. Figures 1−3 show that the coordinated organic fragment in **4** and **5** is located relatively far away from Os(3) whereas in **6** and **7** the coordinated fragment of the organic ligand and Os(3) are spaced by a distance that differs only slightly from that in the pentagonal pyramid framework of **8** and **9**.

Closure of the open structures in **6** and **7** causes substantial changes of the geometrical parameters in relevant parts of **8** and **9**. In particular, the formation of the pentagonal pyramid results in bonding between Os(3) and C(11), C(12), C(13) atoms as well in the further folding of "Os(1)Os(2)Os(3)"−"Os(1)Os(2)C(11)C(12)C(13)" planes. The C(11)−Os(2)−Os(3) and C(13)−Os(1)−Os(3) angles, which are close to 90° in **6** and **7**, have been contracted to 53.1(1)° and 55.2(1)°; 54.5(3)° and 55.6(3)° in **8** and **9**, respectively. Involvement of the formally double C(11)−C(12) (**6**) and C(12)−C(13) (**7**) bonds in formation of the closed cluster framework results in their elongation from 1.374(10) and 1.24(5) Å to 1.425(6) and 1.422(15) Å, in **8** and **9**, respectively; this points to the critical role of the π electrons in this transformation. Considerable changes are also observed in the Os(1)−Os(3) and Os(2)−Os(3) bond lengths, which become shorter because of the bonding requirements of the μ_3-coordinated organic moiety. In contrast, the Os(1)−Os(2) bond, which is bridged by the hydride ligand, is only expanded by 0.0229 and 0.044 Å in **8** and **9**, respectively, to accommodate the increase in the length of the C(11)−C(12)−C(13) chain. The ^{1}H and ^{13}C NMR

spectroscopic data for **8** and **9** are consistent with the structures found in the solid state.

Conclusions

Diyne ligands containing NH groups in β-positions of their substituents easily undergo cyclization reactions with $[H_2Os_3(CO)_{10}]$ to give five-membered pyrrolyl rings coordinated to an edge of the osmium triangle in μ-η^1:η^2- or μ-η^1:η^1-manner. Reactions of $[H_2Os_3(CO)_{10}]$ with $PhC_2C_2CH_2NHPh$ (**1**) and $PhC_2C_2CH_2NHCH_2Ph$ (**2**) give $[HOs_3(CO)_{10}\{\mu\text{-}\eta^1\text{:}\eta^2\text{-}(Ph-(NCHCHCC)-CH_2Ph)\}]$ (**4**) and $[HOs_3(CO)_{10}\{\mu\text{-}\eta^1\text{:}\eta^2\text{-}(PhCH_2-(NCHCHCC)-CH_2Ph)\}]$ (**5**), respectively. Both **4** and **5** contain pyrrolyl rings that are coordinated to edges of the Os_3 triangle in μ-η^1:η^2-coordination modes (σ,π-alkenyl coordination). The third diyne, $PhNHCH_2C_2C_2CH_2NHPh$ (**3**), reacts with $[H_2Os_3(CO)_{10}]$ to give $[HOs_3(CO)_{10}\{\mu\text{-}\eta^1\text{:}\eta^1\text{-}(Ph-(NCHCHCC)-C-CH_3)\}]$ (**6**), which contains a substituted pyrrolyl moiety that is similar to those found in **4** and **5**, although it is bound in a μ-η^1:η^1-coordination mode. Furthermore, the rearrangement of **3** is accompanied by elimination of aniline through C−N bond cleavage in one of the ligand substituents.

A possible reaction scheme for these cyclization reactions incorporate the following features.

1. Hydride transfer from the cluster to the diyne ligand forms an alkenyl cluster. The resultant structural distortion of the initially linear ligand may provide the first step toward further cyclization.

2. The presence of an "active" nucleophilic center in β-position of a substituent of the diyne chain is necessary for formation of a five-membered ring. This also means that a heteroatom (or carbon atom) in the β-position should bear a labile/acidic hydrogen, which may take part in a nucleophilic addition of the X−H group to the unsaturated/coordinated C−C bond in the actual cyclization step.

Clusters containing the μ-η^1:η^1-coordination mode of the organic moiety are thermally unstable and easily undergo CO loss and concomitant transformation of the cluster frameworks. Thus, both **6** and its analogue $[HOs_3(CO)_{10}\{\mu\text{-}\eta^1\text{:}\eta^1\text{-}((OCHCHCC)-C-CH_3)\}]$ (**7**) easily lose a CO ligand during heating in boiling heptane to give the clusters $[HOs_3(CO)_9\{\mu_3,\eta^3\text{-}(Ph-(NCHCHCC)-C-CH_3)\}]$ (**8**) and $[HOs_3(CO)_9\{\mu_3,\eta^3\text{-}((OCHCHCC)-C-CH_3)\}]$ (**9**), respectively, in nearly quantitative yield. The solid-state structures of **8** and **9** reveal that the cluster frameworks of **6** and **7** have been rearranged to give closed pentagonal pyramidal *nido* cluster cores containing three osmium and three carbon atoms.

Acknowledgment. We gratefully acknowledge financial support from INTAS (Grant No 97-3199), the Russian Foundation for Basic Research (Grant No 98-03-32744a), the Royal Swedish Academy of Sciences and Nordic Council of Ministers (I.A.B., V.D.K.), the Wenner-Gren Foundation (S.P.T.), the European Union (TMR network Metal Clusters in Catalysis and Organic Synthesis, E.N. and TP), and the Swedish Technological Sciences Research Council (TFR).

Supporting Information Available: Tables S1−S25, giving a summary of X-ray analysis, atomic coordinates, anisotropic thermal parameters, and bond distances and angles for the structures of clusters **4**, **5**, **6**, **8**, and **9**; Figures S1−S15 of observed and calculated mass spectra for the same compounds. This material is available free of charge via the Internet at http://pubs.acs.org.

OM010400A